Band structure of acoustic waves in phononic lattices: Two-dimensional composites with large acoustic mismatch

Yukihiro Tanaka, Yoshinobu Tomoyasu, and Shin-ichiro Tamura
Department of Applied Physics, Hokkaido University, Sapporo 060-8628, Japan
(Received 30 March 2000)

The finite-difference time-domain method is applied to the calculation of dispersion relations of acoustic waves in two-dimensional (2D) phononic lattices, i.e., periodic solid-solid, solid-liquid, and solid-vacuum composites, for which the conventional plane-wave-expansion method fails or converges very slowly. Numerical examples are developed for 2D structures with polyethylene, mercury, and vacuum cylinders forming a square lattice in an aluminum matrix. The implication of the calculated dispersion relations for ultrasound transmission experiments is discussed.

I. INTRODUCTION

There has been a growing interest in recent years in the study of two-dimensional (2D), periodic, dielectric structures, so-called photonic crystals.[1,2] The existence of complete band gaps (photonic band gaps) of electromagnetic waves in these structures can lead to a variety of phenomena of both fundamental and practical interest. The analogy between photons and phonons suggests the consideration of periodic elastic composites of two or more vibrating materials called phononic crystals or phononic lattices. By appropriate modulation of elastic properties in the constituent materials, forbidden frequency gaps (acoustic stop bands) extending throughout the Brillouin zone can also be realized.[3–6] A possible application of such phononic crystals is designing phonon filters or heat insulators, which selectively reflect phonons in desirable frequency ranges.

To probe the acoustic band structure of these composites, ultrasound transmission experiments in both the bulk and on the surface of the structures have been performed.[7–12] The dimension of the phononic crystals used in the experiments is typically in the range of millimeters and a composite structure is made by drilling in a solid substrate a periodic array of cylinders. The simplest structure should be the one with vacuum or air-filled cylindrical holes. Intuitively, these holes should scatter acoustic waves strongly, and the transmission of ultrasound through the structure is expected to be small or even prohibited for a large cross section of the cylinders. Another interesting and still easily accessible structure is that of cylinders filled with a liquid[7] or a low-melting-point polymer[12] (which may solidify at room temperatures). These composites are characterized by a large acoustic mismatch between the cylinder and substrate materials, or by the fact that two modes of acoustic waves (transverse modes) are not allowed to exist in the cylinders.

So far, several authors have calculated acoustic band structures of 2D phononic crystals for both the bulk[3–6] and surface[13,14] vibrations with a plane-wave-expansion (PWE) method. This simple method usually works very well. However, within this framework a large number of plane waves is required to obtain a reliable band structure for a composite of elastic media with a large acoustic mismatch. Moreover, if the cylinder material is a nonviscous fluid (or vacuum) which does not support the propagation of transverse (or both the transverse and longitudinal) waves, the PWE fails by producing unphysical flat frequency bands. Thus more efficient methods beyond the PWE scheme are necessary for the calculation of the dispersion relations in some interesting phononic crystals.

The purpose of the present study is to calculate realistic dispersion relations of phonons in a variety of 2D phononic crystals for which the conventional PWE method is not applicable. This is carried out by solving the elastic wave equations by the finite-difference time-domain (FDTD) method.[15–17] The FDTD method is a popular numerical scheme for the solution of many problems in electromagnetics. It is especially effective for a large-scale simulation of a finite complex system, and has recently been applied to the study of both the transmission and frequency spectra of electromagnetic waves in photonic crystals. (Very recently, this scheme has been applied to the calculation of transmission rates in 3D-phononic crystals.[18]) More explicitly, we calculate the acoustic band structures of the 2D elastic composites consisting of cylinders of a solid, fluid, or vacuum arranged periodically in an aluminum substrate. The results obtained are compared with the published ultrasound transmission experiments.

II. FORMULATION

A. Finite-difference time-domain (FDTD) method

We consider 2D composite structures consisting of a periodic array of cylinders (denoted by A) embedded in a background elastic material (denoted by B). The cylinder material A can be an elastic medium like a solid or liquid, or just vacuum. The equation governing the motion of lattice displacement $\mathbf{u}(\mathbf{r},t)$ in this inhomogeneous system is given by

$$\rho(\mathbf{x})\ddot{u}_i(\mathbf{r},t)=\partial_j\sigma_{ij}(\mathbf{r},t), \tag{1}$$

$$\sigma_{ij}(\mathbf{r},t)=c_{ijmn}(\mathbf{x})\partial_n u_m(\mathbf{r},t), \tag{2}$$

where $\mathbf{r}=(\mathbf{x},z)=(x,y,z)$ (the z axis is taken to be parallel to the cylinder axis), $\rho(\mathbf{x})$ and $c_{ijmn}(\mathbf{x})$ are the position-dependent mass density and elastic stiffness tensor of the

system, respectively, and $\sigma_{ij}(\mathbf{r},t)$ is the stress tensor. Note that ρ and c_{ijmn} do not depend on z because of the homogeneity of the system along the cylinder axis. The summation convention over repeated indices is assumed in the present paper.

For the propagation of bulk acoustic waves in the $\mathbf{x}$ plane normal to the axis of the cylinders, we may find solutions homogeneous in the z direction, i.e., $u_i(\mathbf{r},t)=u_i(\mathbf{x},t)$ and $\sigma_{i,j}(\mathbf{r},t)=\sigma_{i,j}(\mathbf{x},t)$. Owing to the periodicity within the $\mathbf{x}$ plane, the lattice displacement and the stress tensor take the forms satisfying the Bloch theorem

$$u_i(\mathbf{x},t)=e^{i\mathbf{k}\cdot\mathbf{x}}U_i(\mathbf{x},t), \tag{3}$$

$$\sigma_{ij}(\mathbf{x},t)=e^{i\mathbf{k}\cdot\mathbf{x}}S_{ij}(\mathbf{x},t), \tag{4}$$

where $\mathbf{k}=(k_x,k_y)$ is a Bloch wave vector and $\mathbf{U}(\mathbf{x},t)$ and $S_{ij}(\mathbf{x},t)$ are periodic functions satisfying $\mathbf{U}(\mathbf{x}+\mathbf{a},t)=\mathbf{U}(\mathbf{x},t)$ and $S_{ij}(\mathbf{x}+\mathbf{a},t)=S_{ij}(\mathbf{x},t)$ with $\mathbf{a}$ a lattice translation vector. Thus Eqs. (1) and (2) are rewritten as

$$\rho(\mathbf{x})\ddot{U}_i(\mathbf{x},t)=ik_jS_{ij}(\mathbf{x},t)+\partial_jS_{ij}(\mathbf{x},t), \tag{5}$$

$$S_{ij}(\mathbf{x},t)=c_{ijmn}(\mathbf{x})[ik_nU_m(\mathbf{x},t)+\partial_nU_m(\mathbf{x},t)]. \tag{6}$$

Now we try to solve these equations with respect to the reduced fields $U_i(\mathbf{x},t)$ and $S_{ij}(\mathbf{x},t)$ within a unit cell of the structure.

First we specify a 2D wave vector $\mathbf{k}$ in the first Brillouin zone. Once appropriate initial and boundary conditions are specified, Eqs. (5) and (6) can be solved numerically for each normal mode by discretizing both the time and space domains. [The explicit expressions for the discretized versions of Eqs. (5) and (6) are given in the Appendix.] More explicitly, when the displacement fields are specified at an instant $t=0$, their spatial derivatives are determined using simple finite-difference formulas. Equations (5) and (6) then give us the time derivative of the displacement field $\mathbf{U}$, which allows us to update $\mathbf{U}(\mathbf{x},t)$ for small but positive t. In this way, the displacement fields $\mathbf{U}(\mathbf{x},t_i)$ at discretized points on the time axis t_i $(i=1,2,\ldots)$ are determined for many 2D grid points sampled in the $\mathbf{x}$ plane. For a sufficiently large number of these $\mathbf{U}$ data on the time axis, the displacement fields are Fourier-transformed into the frequency space. The positions of the existing peaks in the frequency spectra are then identified as the eigenfrequencies of the normal vibrational modes for a given wave vector $\mathbf{k}$.

B. Plane-wave expansion (PWE) method

For comparison we also briefly recapitulate the PWE method for solving the wave equations (1) and (2). In this scheme we expand the position-dependent quantities as

$$\mathbf{u}(\mathbf{x},t)=\sum_{\mathbf{G}} e^{i(\mathbf{k}+\mathbf{G})\cdot\mathbf{x}-i\omega t}\mathbf{a}_{\mathbf{G}}, \tag{7}$$

$$\rho(\mathbf{x})=\sum_{\mathbf{G}} e^{i\mathbf{G}\cdot\mathbf{x}}\rho_{\mathbf{G}}, \tag{8}$$

$$c_{ijmn}(\mathbf{x})=\sum_{\mathbf{G}} e^{i\mathbf{G}\cdot\mathbf{x}}c_{\mathbf{G}}^{ijmn}, \tag{9}$$

where $\mathbf{G}=(G_x,G_y)$ is a 2D reciprocal-lattice vector and ω is an angular frequency. The Bloch theorem is again used for the displacement vector $\mathbf{u}$ in Eq. (7). For a square lattice where circular cylinders of radius r_0 are embedded periodically in a background material with spacing a, the reciprocal-lattice vector is $\mathbf{G}=(2\pi N_1/a,2\pi N_2/a)$ with N_1 and N_2 integers. The Fourier coefficients of the mass density and elastic stiffness tensors are thus given by

$$\alpha_{\mathbf{G}}=\begin{cases} f\alpha_A+(1-f)\alpha_B & \text{for } \mathbf{G}=0, \\ (\alpha_A-\alpha_B)F(\mathbf{G}) & \text{for } \mathbf{G}\neq 0, \end{cases} \tag{10}$$

where $\alpha=(\rho,c^{ijmn})$, $f=\pi r_0^2/a^2$ (the maximum value is $f_{\max}=\pi/4=0.785$) is the filling fraction which defines the cross-sectional area of a cylinder relative to the unit-cell area, and

$$F(\mathbf{G})=\frac{2fJ_1(|\mathbf{G}|r_0)}{|\mathbf{G}|r_0} \tag{11}$$

with $J_1(x)$ a Bessel function. Thus truncating the expansions (7)–(9) by keeping $N\times N=N^2$ reciprocal-lattice vectors (i.e., N^2 plane waves), Eq. (7) gives $3N^2$ eigenfrequencies $\omega=\omega_l$ $(l=1-3N^2)$ for a given 2D wave vector $\mathbf{k}$.

III. NUMERICAL EXAMPLES

For the propagation of acoustic waves in the $\mathbf{x}$ plane normal to the axis of cylinders (the z axis), the wave polarized in the z direction [a transverse (T) wave] is decoupled from the other two modes [the other T and longitudinal (L) modes] of the waves polarized in the $\mathbf{x}$ plane. We call the former mode of the wave the ''single'' mode and the latter two modes coupled to each other the ''mixed'' mode. In the numerical calculation, polycrystalline aluminum (elastically isotropic) is assumed for the background material (B) and we consider three kinds of 2D lattices with the cylinders (A) filled with (i) polyethylene (a soft solid), (ii) mercury (liquid), and (iii) vacuum, respectively.[19] In the FDTD scheme for wave propagation, we divide the unit cell of a 2D square lattice into a grid of $n\times n$ $(n=100-200)$ points and simulate the time evolution over $2^{19}(=524\,288)-2^{20}(=1\,048\,576)$ time steps with each time step $0.003a/v_t$, where v_t is the sound velocity of the transverse mode in the background material.

A. Polyethylene/Al lattices

First we consider a 2D polyethylene/Al square lattice. The PWE method is still applicable to this lattice but its convergence is slow. Figure 1 illustrates the FDTD (dots) and PWE (solid lines) calculations of the dispersion relations for the acoustic waves along the boundary of the irreducible part of the Brillouin zone ($f=0.4$). Only frequencies of the mixed mode are plotted. The FDTD scheme assumes a grid of $n\times n=120^2$ points in a unit cell and the PWE method assumes $N\times N=41^2=1681$ plane waves, or reciprocal lattice vectors. The latter results lie slightly above the frequencies obtained by the FDTD scheme. A large acoustic mismatch between polyethylene (PE) and aluminum ($Z_{\mathrm{PE}}/Z_{\mathrm{Al}}=0.1$ for the longitudinal mode)[19] makes the convergence of the PWE calculation very slow, as shown in the inset of Fig. 1. This is mainly due to the fact that a large number of plane waves is

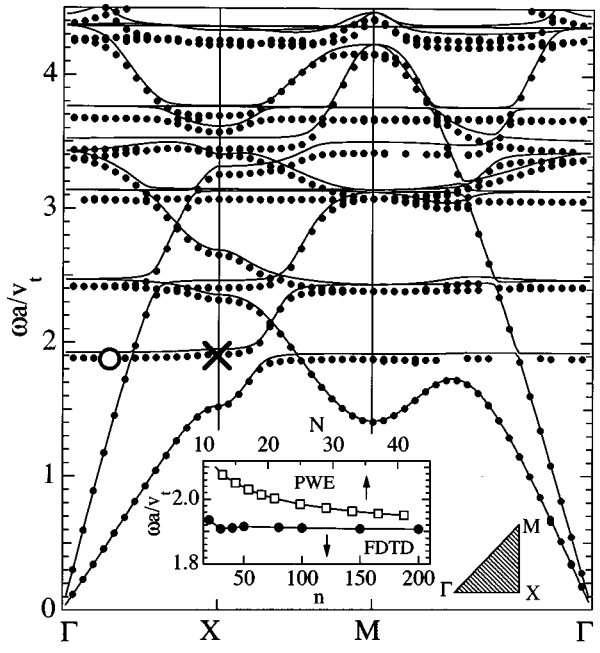

FIG. 1. Dispersion relations of the mixed modes (the coupled longitudinal and transverse acoustic waves) in a two-dimensional square lattice consisting of polyethylene cylinders in an Al substrate with filling fraction $f=0.4$. ($v_t=3.11\times10^5$ cm/s is the transverse sound velocity in Al and a is the lattice spacing.) Dots and solid lines are the FDTD (with a grid of $n\times n=120^2$ points in a unit cell) and PWE (with $N\times N=41^2$ plane waves) calculations, respectively. The wave-vector direction is perpendicular to the cylinder axis. The inset compares the convergence of both the FDTD (dots) and PWE (open squares) calculations for the frequency marked by the cross on the flat branch at the X point. The irreducible part of the Brillouin zone is also displayed.

required [in the expansions (8) and (9)] to reproduce the spatial profiles of the mass density and elastic constants changing abruptly in space. In contrast, the FDTD calculation is substantially converged for n as large as $n=50$. The CPU times to calculate eigenfrequencies for a given wave vector are typically 160 sec for the FDTD scheme with $n=41$ and with 2^{19} time steps, and 320 sec for the PWE method with $N=41$ on a HITACHI SR8000 supercomputer.

In Fig. 1, we observe no complete gap in the frequency range plotted in spite of the large acoustic mismatch between the constituent materials and also the large filling fraction f assumed. A remarkable feature of the dispersion relation in this lattice is the appearance of a number of optical-like flat branches. The existence of these flat branches is another characteristic feature of a composite structure constituted from materials with a large acoustic mismatch.[6] At frequencies on these branches, lattice vibrations are localized in the elastically softer medium (polyethylene) which fills the cylinders. As shown in Fig. 2, the amplitude of vibration is well concentrated at the positions of the cylinders and it is very small in the substrate medium. We expect that the transmission of an acoustic wave is resonantly enhanced when its frequency coincides with one of these branches. At the same time, a large time delay should accompany the transmission.[20] Unfortunately, there is no ultrasound transmission experiment to be compared with these calculated frequency spectra.

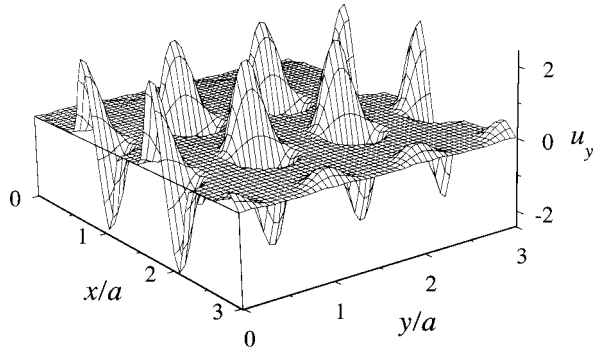

FIG. 2. Pseudo-three-dimensional representation of the lattice displacement u_y (the component perpendicular to the cylindrical axis) in the polyethylene/Al phononic lattice, same as for Fig. 1. The selected wave vector and frequency ($\omega a/v_t=1.92$) are those corresponding to the point indicated by the open circle in Fig. 1 (a point on a flat branch). The center of the cylinders are located at (ma,na), where m and n are integers.

B. Hg/Al lattices

If the cylinders embedded in a solid substrate are filled with nonviscous liquid, the simple PWE method for calculating acoustic-wave dispersion relations fails. This is because a transverse vibration does not exist inside a liquid, but the conventional PWE method still assumes a finite displacement amplitude for this vibrational mode in the cylinders. The calculated dispersion relation for the mixed mode (inset of Fig. 3, for example) exhibits many flat branches like the ones in the preceding subsection. But in this lattice they are fictitious. This can be seen from the fact that the number of

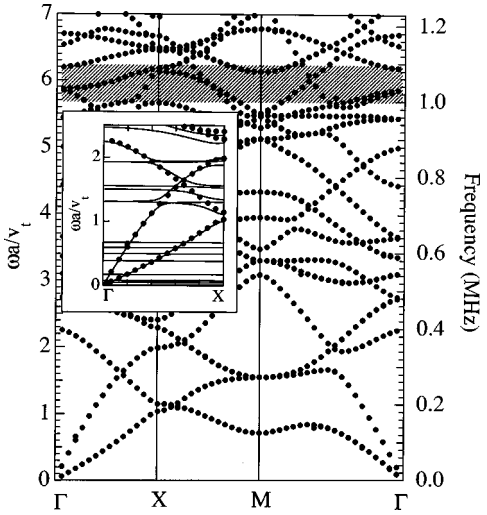

FIG. 3. FDTD results (with a grid of $n\times n=120^2$ points in a unit cell) for the dispersion relations of the mixed modes (coupled longitudinal and transverse acoustic waves) in a two-dimensional square lattice consisting of mercury circular cylinders in an Al substrate with filling fraction $f=0.4$. ($v_t=3.11\times10^5$ cm/s is the transverse sound velocity in Al and a is the lattice spacing.) Hatched region is the frequency range where large transmission dips are observed for the longitudinal sound (Ref. 6). Inset compares the frequencies obtained by the FDTD calculation (dots) and the PWE method (solid lines) with $N\times N=11^2$ plane waves in the $\Gamma-X$ direction.

flat branches increases as the number of plane waves kept in the PWE calculation is increased. We have already shown that at a frequency on a flat branch, the amplitude in the softer material is much larger than that in the harder material. In the present structure the amplitude of transverse vibrations obtained by the PWE scheme is finite inside the cylinders but effectively zero outside at a frequency in a flat branch. Evidently this is physically unacceptable. In contrast, the FDTD calculation gives dispersion relations free of such flat branches as shown in Fig. 3 for the mixed longitudinal and transverse modes. The real structure of the dispersion curves obtained by the FDTD method is recognized only indistinctly in the PWE calculation.

An ultrasonic transmission experiment of the longitudinal mode with a 2D phononic lattice has been done by Espinosa *et al.* with a structure consisting of an aluminum alloy plate with a square periodic arrangement of cylindrical holes filled with mercury.[7] Transmission dips are found in certain frequency ranges, e.g., 0.6–1.1 MHz in the [100] direction ($\Gamma - X$ direction) for $f=0.4$. A similar measurement in the [110] direction ($\Gamma - M$ direction) suggests the existence of a full band gap (extending from 1.0 to 1.1 MHz) for longitudinal ultrasound in the Hg/Al square lattice. Unexpectedly, in the frequency range suggested by the experiment no complete frequency gap is found in the calculated dispersion relations of the mixed mode which contains the longitudinal polarization. This does not necessarily mean that the longitudinal sound in the above frequency range can propagate through this lattice. For the branches existing in the claimed frequency range, we have to carefully check the polarization of the waves. This is, however, beyond the scope of the present work. Evidently, a direct calculation of the transmission rate is necessary to resolve this apparent discrepancy. The FDTD calculation of the transmission will appear elsewhere.

It should also be noted that the amalgam of the mercury and aluminum might be formed at the boundaries of the Hg cylinders and Al background of the structure. If this is indeed the case, the transition regions of a finite thickness should exist near the boundary of the cylinders for both the density and elastic constants and thus the filling fraction f may be changed effectively. The consideration of such effects will also be interesting.

C. Vacuum/Al lattices

If nothing is filled in the cylinders, acoustic waves propagate in a 2D phononic lattice only through the substrate material. This means that the acoustic wave with a given wave vector is scattered strongly from the cylinder surfaces as the filling fraction f increases. Thus acoustic stop bands extending over entire region of the Brillouin zone are expected to appear for some range of f.

The dispersion relations of both the mixed (filled circles) and single (open circles) modes calculated by the FDTD method (with a grid of $n\times n=200^2$ points in a unit cell) are shown in Fig. 4 for a 2D vacuum/Al lattice for $f=0.55$ ($r_0/a=0.42$). We really find the existence of a complete frequency gap which prohibits the propagation of all three polarizations simultaneously in any direction. The width of this complete gap is plotted in the inset as a function of the filling fraction f. The gap width $\Delta\omega$ increases almost monotonically with f for both the mixed L-T and single T modes.

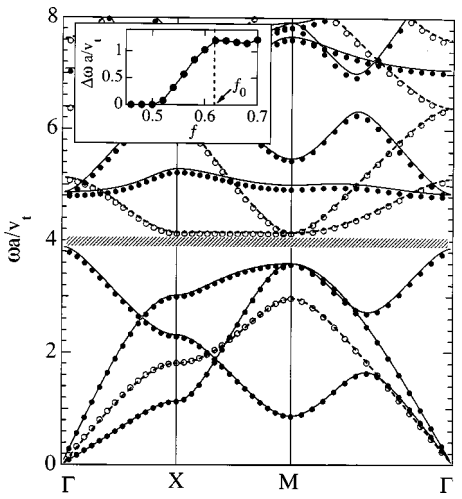

FIG. 4. FDTD results (with a grid of $n\times n=200^2$ points in a unit cell) for the dispersion relations of the coupled longitudinal and transverse modes (dots) and the single transverse mode (open circles) in a two-dimensional square lattice consisting of vacuum circular cylinders in an Al substrate with filling fraction $f=0.55$. ($v_t=3.11\times10^5$ cm/s is the transverse sound velocity in Al and a is the lattice spacing.) Also plotted by the solid and dashed lines are the PWE calculations (with $N\times N=41^2$ plane waves) for the coupled and single modes, respectively. The hatched region shows the complete gap for three acoustic modes. The inset shows the width $\Delta\omega$ of the complete gap versus filling fraction f. For $f>f_0=0.62$ (the vertical dashed line), the gap width is determined by the highest frequency of the single mode in the first band and the lowest frequency of the mixed mode in the second band. For $f<f_0$, it is determined by the highest and lowest frequencies of the mixed mode in the first and the second bands.

An interesting observation is the fact that the PWE method is applicable with some manipulation to the calculation of the dispersion relations for a 2D phononic lattice with vacuum cylinders. In this lattice both the mass density and elastic constants are zero in the cylinder regions. A question is how to take the limits ρ_A, $c_A^{ijmn}\rightarrow 0$, in cylinders (A) in the framework of the PWE method. (In the FDTD scheme, no elastic medium is assumed at the grid points inside the cylinders.) If we take these limits by assuming $\rho_A/c_A^{ijmn}\rightarrow 0$, the dispersion curves obtained (with $N\times N=41^2$ plane waves) are those displayed in Fig. 4 by the solid (for the mixed mode) and dashed (for the single mode) lines, respectively. The agreement between the FDTD and PWE results is excellent. Here we note that the spurious flat branches of both the longitudinal and transverse modes expected to appear in the PWE calculation are now pushed out to the very high-frequency region. Thus they do not interact with real branches of the system at a finite frequency range. This is quite different from the case for the PWE calculation applied to the liquid/solid lattice (the preceding subsection), where the mass density of the liquid (cylinder material) is not a disposal parameter and the flat branches stay at the finite frequency region.

IV. CONCLUDING REMARKS

In the present work we have calculated the dispersion relations of the bulk acoustic waves in 2D phononic lattices consisting of periodic arrays of circular cylinders embedded in a background substance. The lattices considered are those with a large acoustic mismatch between their constituent materials, and also the cases where the transverse or both the longitudinal and transverse modes of vibrations do not exist inside cylinders. For these lattices the conventional PWE method for the calculation of the dispersion relations is usually not very reliable and an alternative approach is required. The numerical approach based on the FDTD method is proved to be very efficient for these cases.

Contrary to the recent ultrasound transmission experiment,[7] no complete frequency gap is found in the claimed region of a 2D square phononic lattice with mercury cylinders embedded in an aluminum matrix. The polarization of the branches found in this frequency region is important for a comparison of the transmission and frequency spectra. For a more direct comparison, the calculation of the transmission rate is necessary. For photonic crystals, the theoretical transmission rate of electromagnetic waves has been given by Sakoda[21] with the PWE method and also by Fan *et al.*[22] with the FDTD method. A similar calculation of the transmission rate with the FDTD method is currently underway for phononic lattices.

Another interesting subject is the calculation of the band structure of surface acoustic waves in 2D phononic crystals. The distribution of the frequency band of surface acoustic waves is usually well separated from those of bulk waves, and their stop-band distribution has been observed by both surface wave transmission and imaging experiments.[11,12] An attenuation associated with the Rayleigh surface wave propagation has been measured in a 2D triangular and honeycomb (hexagonal) lattice with vacuum cylinders drilled in a marble quarry[11] and also with polymer cylinders drilled in an aluminum substrate.[12] The attenuation in transmission spectra in the former lattice suggests the existence of absolute band gaps for the surface waves. However, the measurements are sometimes compared with a theoretical calculation with a simple scalar-wave model. We also plan to apply the FDTD method for the calculation of the dispersion relation of surface localized vibrations in 2D periodic structures.

ACKNOWLEDGMENTS

This work was supported in part by a Grant-in-Aid for Scientific Research from the Ministry of Education, Science and Culture of Japan (Grant No. 09640385).

APPENDIX A

In this appendix, we give the explicit expressions for the discretized versions of Eqs. (5) and (6):

$$\frac{\rho^{l,m}}{(\Delta t)^2}[U_1^{l,m;n+1}-2U_1^{l,m;n}+U_1^{l,m;n-1}] = K_1^+ S_{11}^{l+(1/2),m;n}+K_1^- S_{11}^{l-(1/2),m;n} + K_2^+ S_{12}^{l,m+(1/2);n}+K_2^- S_{12}^{l,m-(1/2);n}, \quad \text{(A1)}$$

$$\frac{\rho^{l+(1/2),m+(1/2)}}{(\Delta t)^2}[U_2^{l+(1/2),m+(1/2);n+1}-2U_2^{l+(1/2),m+(1/2);n} + U_2^{l+(1/2),m+(1/2);n-1}] = K_1^+ S_{21}^{l+1,m+(1/2);n}+K_1^- S_{21}^{l,m+(1/2);n} + K_2^+ S_{22}^{l+(1/2),m+1;n}+K_2^- S_{22}^{l+(1/2),m;n}, \quad \text{(A2)}$$

$$S_{11}^{l+(1/2),m;n} = C_{11}^{l+(1/2),m}[K_1^+ U_1^{l+1,m;n}+K_1^- U_1^{l,m;n}] + C_{12}^{l+(1/2),m}[K_2^+ U_2^{l+(1/2),m+(1/2);n} + K_2^- U_2^{l+(1/2),m-(1/2);n}], \quad \text{(A3)}$$

$$S_{22}^{l+(1/2),m;n} = C_{12}^{l+(1/2),m}[K_1^+ U_1^{l+1,m;n}+K_1^- U_1^{l,m;n}] + C_{11}^{l+(1/2),m}[K_2^+ U_2^{l+(1/2),m+(1/2);n} + K_2^- U_2^{l+(1/2),m-(1/2);n}], \quad \text{(A4)}$$

$$S_{12}^{l,m+(1/2);n} = S_{21}^{l,m+(1/2);n} = C_{44}^{l,m+(1/2)}[K_1^+ U_2^{l+(1/2),m+(1/2);n} + K_1^- U_2^{l-(1/2),m+(1/2);n}+K_2^+ U_1^{l,m+1;n} + K_2^- U_1^{l,m;n}], \quad \text{(A5)}$$

where (l,m) defines a 2D grid point (grid spacings are Δx and Δy), n specifies the time step with an interval Δt, and $K_1^{\pm}=(k_x\Delta x\pm 2)/2\Delta x$ and $K_2^{\pm}=(k_y\Delta y\pm 2)/2\Delta y$. In the above equations, the coefficients C_{ij} are related to the elastic stiffness tensor c_{ijmn} in a usual manner. The initial conditions (the displacement fields at $t=0$) are chosen such that $U_1^{l,m;0}=\delta_{l,l_0}\delta_{m,m_0}$ and $U_2^{l+1/2,m+1/2;0}=0$, where the 2D grid point (l_0,m_0) is selected at random in the unit cell.

[1] *Photonic Band Gaps and Localization*, edited by C. M. Soukoulis (Plenum, New York, 1993).
[2] J. D. Joannopoulos, R. D. Meade, and J. N. Winn, *Photonic Crystals* (Princeton Univ. Press, Princeton, 1995).
[3] M. S. Kushwaha, P. Halevi, L. Dobrzynski, and B. D. -Rouhani, Phys. Rev. Lett. **71**, 2022 (1993).
[4] M. S. Kushwaha, P. Halevi, G. Martinez, L. Dobrzynski, and B. D. -Rouhani, Phys. Rev. B **49**, 2313 (1994).
[5] M. Sigalas and E. N. Economou, Solid State Commun. **86**, 141 (1993).
[6] J. O. Vasseur, B. Djafari-Rouhani, L. Dobrzynski, M. S. Kushwaha, and P. Halevi, J. Phys.: Condens. Matter **6**, 8759 (1994).
[7] F. R. Montero de Espinosa, E. Jiménez, and M. Torres, Phys. Rev. Lett. **80**, 1208 (1998).
[8] J. O. Vasseur, P. A. Deymier, G. Frantziskonis, G. Hong, B. Djafari-Rouhani, and L. Dobrzynski, J. Phys.: Condens. Matter

10, 6051 (1998).
[9] M. Torres, F. R. Montero de Espinosa, D. García-Pablos, and N. García, Phys. Rev. Lett. **82**, 3054 (1999).
[10] J. V. Sánchez-Pérez *et al.*, Phys. Rev. Lett. **80**, 5325 (1998).
[11] F. Meseguer *et al.*, Phys. Rev. B **59**, 12 169 (1999).
[12] R. E. Vines, J. P. Wolfe, and A. G. Every, Phys. Rev. B **60**, 11 871 (1999).
[13] Y. Tanaka and S. Tamura, Phys. Rev. B **58**, 7958 (1998).
[14] Y. Tanaka and S. Tamura, Phys. Rev. B **60**, 13 294 (1999).
[15] A. Taflove, *Advances in Computational Electrodynamics: The Finite-Difference Time-Domain Method*, edited by C. M. Soukoulis (Artech House, London, 1998).
[16] C. T. Chan, Q. L. Yu, and K. M. Ho, Phys. Rev. B **51**, 16 635 (1995).
[17] A. J. Ward and J. B. Pendry, Phys. Rev. B **58**, 7252 (1998).
[18] M. Sigalas and N. Garcia, J. Appl. Phys. **87**, 3122 (2000).
[19] We use the elastic constants (in units of 10^{10} dyn/cm^2) $C_{\mathrm{Al}}^{11}=110.9$ and $C_{\mathrm{Al}}^{44}=26.1$ for aluminum, $C_{\mathrm{PE}}^{11}=3.42$ and $C_{\mathrm{PE}}^{44}=0.262$ for polyethylene, $C_{\mathrm{Hg}}^{11}=28.6$ and $C_{\mathrm{Hg}}^{44}=0$ for mercury, and $C_I^{12}=C_I^{11}-2C_I^{44}$ for $I=$ Al, PE, and Hg. The mass densities are $\rho_{\mathrm{Al}}=2.7$ g cm^{-3} for aluminum, $\rho_{\mathrm{PE}}=0.9$ g cm^{-3} for polyethylene, and $\rho_{\mathrm{Hg}}=13.6$ g cm^{-3} for mercury. The longitudinal sound velocities used are $v_{\mathrm{Al}}=6.41\times10^5$ cm s^{-1} for aluminum, $v_{\mathrm{PE}}=1.95\times10^5$ cm s^{-1} for polyethylene, and $v_{\mathrm{Hg}}=1.45\times10^5$ cm s^{-1} for mercury.
[20] S. Mizuno and S. Tamura, Phys. Rev. B **50**, 7708 (1994).
[21] K. Sakoda, Phys. Rev. B **51**, 4672 (1995); **52**, 8992 (1995).
[22] S. Fan, P. R. Villeneuve, and J. D. Joannopoulos, Phys. Rev. B **54**, 11 245 (1996).